JPE 17-6-18

https://doi.org/10.6113/JPE.2017.17.6.1577
ISSN(Print): 1598-2092 / ISSN(Online): 2093-4718

A Fuzzy Self-Tuning PID Controller with a Derivative Filter for Power Control in Induction Heating Systems

Arijit Chakrabarti[†], Avijit Chakraborty[*], and Pradip Kumar Sadhu[*]

[†,*]Department of Electrical Engineering, Indian Institute of Technology (ISM), Dhanbad, India

Abstract

The Proportional-Integral-Derivative (PID) controller is still the most widespread control strategy in the industry. PID controllers have gained popularity due to their simplicity, better control performance and excellent robustness to uncertainties. This paper presents the optimal tuning of a PID controller for domestic induction heating systems with a series resonant inverter for controlling the induction heating power. The objective is to design a stable and superior control system by tuning the PID controller with a derivative filter (PIDF) through Fuzzy logic. The paper also compares the performance of the Fuzzy PIDF controller with that of a Ziegler-Nichols PID controller and a fine-tuned PID controller with a derivative filter. The system modeling and controllers are simulated in MATLAB/SIMULINK. The results obtained show the effectiveness and superiority of the proposed Fuzzy PID controller with a derivative filter.

Key words: Induction heating, Inverter, Self-tuning, Simulation

I. INTRODUCTION

Induction heating has become one of the preferred heating technologies in industrial, domestic and medical applications due to its advantages over classical heating techniques such as flame heating, resistance heating as well as traditional ovens and furnaces [1]. It uses power semiconductor devices with high-frequency switching ranging from 20 kHz to 100 kHz.

The evolution of domestic induction heating technology increasingly demands sophisticated control algorithms that are capable of providing robust performance without dependence on variation of the induction load. In recent years, induction cooking has been focusing on the development of control strategies by using high switching frequencies with series resonant inverters and parallel quasi resonant inverters [2], [3] to eliminate the switching loss of semiconductor devices through soft switching or zero-voltage-switching (ZVS).

The output power of the inverters is controlled by adopting various control methods. The Proportional-Integral-Derivative (PID) controller is widely used in induction heating systems. Better reliability, stability and a simple structure have made it suitable for such systems. PID controllers are tuned mostly based on a small amount of information on the dynamic behavior of systems and often do not provide good tuning, resulting in poor control [4]. The PID controller has been designed using the Ziegler-Nichols frequency response method and its performance has been observed.

With conventional PID controller, it is difficult to achieve desired control results. The Ziegler-Nichols (ZN) PID controller parameters are further tuned with a derivative filter to design a PIDF controller for induction heating systems to get satisfactory closed loop performance around its power control. Furthermore, fuzzy logic has been used to set the control parameters of the PID controller to accomplish a self-tuned Fuzzy PIDF power controller for induction heating systems. The performances of a ZN PID controller, a Fine tuned PIDF controller and a Fuzzy PIDF controller have been studied in this paper. The fuzzy PIDF controller appears to be a better controller for induction heating systems.

This paper is organized as follows. Section II introduces the architecture and system configuration of an induction heating system. Section III discusses the design of the controllers. Section IV presents some simulation results. Section V covers

Manuscript received Aug. 11, 2016; accepted Aug. 8, 2017
Recommended for publication by Associate Editor Sung-Jin Choi.
[†]Corresponding Author: a.chakra2010@gmail.com
Tel: +91-90-516-00052, Indian Institute of Technology (ISM)
[*]Dept. of Electrical Eng., Indian Institute of Technology (ISM), India

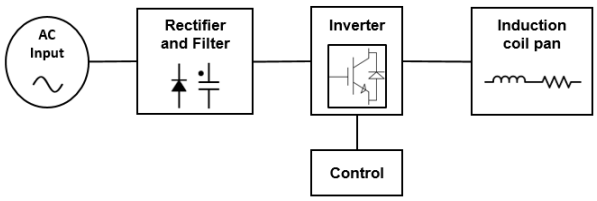

Fig. 1. Typical induction heating system.

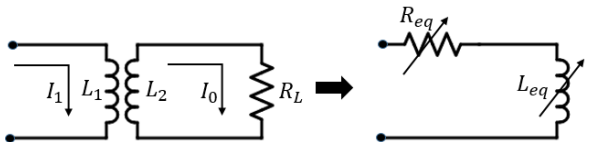

Fig. 2. Equivalent circuit of the load.

experimental verification. Finally, this paper is concluded in section VI.

II. System Configuration

Fig. 1 represents a typical induction heating system. The main power source provides energy to the induction coil-pan. The AC input voltage is rectified by the uncontrolled rectifier comprising four diodes. It converts an alternating current (AC) to a direct current (DC) that is filtered by the DC link capacitor and is fed to the inverter [5].

The induction coil receives a high-frequency current from the inverter to generate an alternating magnetic field that induces eddy currents and causes the hysteresis effect to heat up the material on the pan or cooking vessel. The cooking vessel is made of ferromagnetic materials to achieve a higher efficiency of the electromagnetic coupling when compared to non-ferromagnetic materials. The load circuit consists of a vessel and a coil which can be modeled as a transformer with a single turn secondary winding with an equivalent circuit comprising an inductor L_{eq} and a resistor R_{eq} in series connection, as shown in Fig. 2.

The equivalent load variation depends on various parameters such as coil shape, cooking vessel materials, spacing between the induction coil and the cooking vessel, temperature, excitation frequency, etc.

A full bridge series resonant inverter (SRI) has been selected for the induction heating system considered in this paper since it is one of the most popular resonant inverters and it offers more control options [6]. Fig. 3 shows a serially compensated inverter topology. It comprises four controllable switches (S_1 to S_4) using IGBTs with ultrafast soft recovery diodes (D_1 to D_4) and a series resonant circuit load with an equivalent resistor (R_{eq}), inductor (L_{eq}) and resonant capacitor (C_r). The topology is fed by a voltage source V which can be fixed or variable. All of the switches are operated at a high switching frequency with the switching period T_s. Here, the series resonant circuit load represents an inductive load.

The simplified inverter circuit is shown in Fig. 4 and it can

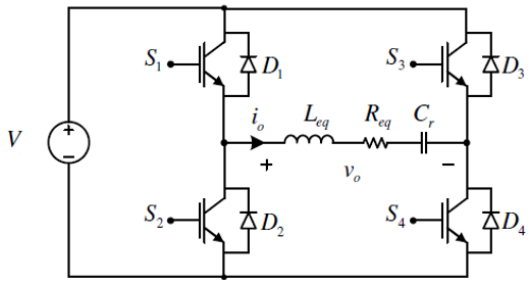

Fig. 3. Full bridge SRI for an induction heater.

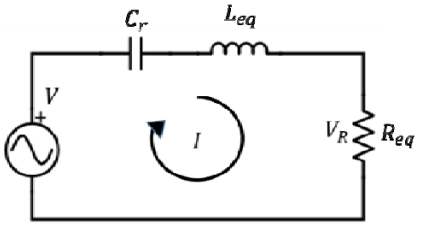

Fig. 4. Simplified inverter circuit.

be leveraged to calculate the voltage transfer function since it is directly related to the power injected to the heating system.

If Kirchhoff's law is applied to the above circuit and the direct Laplace Transform is taken, the following is obtained:

$$V(s)-\frac{I(s)}{sC_r}-sL_{eq}I(s)-R_{eq}I(s)=0 \tag{1}$$

$$V_R(s)=R_{eq}I(s) \tag{2}$$

Arranging the terms and normalizing the above two equations result in:

$$V_R(s)=\frac{\frac{sR_{eq}}{L_{eq}}}{s^2+\frac{sR_{eq}}{L_{eq}}+\frac{1}{L_{eq}C_r}}V(s) \tag{3}$$

The roots of the denominator of the above equation can be expressed as:

$$s=-\frac{R_{eq}}{2L_{eq}}\pm\sqrt{\left(\frac{R_{eq}}{2L_{eq}}\right)^2-\frac{1}{L_{eq}C_r}} \tag{4}$$

It is desired that the system has an oscillatory (under-damped) response since the control system mostly locks it to this natural frequency. Hence, the roots must be complex and need to satisfy the following condition:

$$\left(\frac{R_{eq}}{2L_{eq}}\right)^2<\frac{1}{L_{eq}C_r} \tag{5}$$

Under this condition, Equ. (3) can be written as:

$$V_R(s)=\frac{\frac{sR_{eq}}{L_{eq}}}{\left((s+\alpha)^2+\omega^2\right)}V(s) \tag{6}$$

where:

$$\alpha=\frac{R_{eq}}{2L_{eq}} \tag{7}$$

$$j\omega = \sqrt{\left(\frac{R_{eq}}{2L_{eq}}\right)^2 - \frac{1}{L_{eq}C_r}} \tag{8}$$

The voltage transfer function is given by Equ. (9).

$$\frac{V_R(s)}{V(s)} = \frac{\frac{sR_{eq}}{L_{eq}}}{\left((s+\alpha)^2+\omega^2\right)} \tag{9}$$

The Quality factor (Q) and angular resonant frequency (ω_r) are given by:

$$Q = \frac{\omega_r L_{eq}}{R_{eq}} \tag{10}$$

$$\omega_r = \frac{1}{\sqrt{L_{eq}C_r}} \tag{11}$$

The series CLR circuit acts as a filter. It eliminates the impact for all of the harmonics except the first one. Therefore, for analysis, only the first harmonic is considered in this paper. The source voltage is defined as:

$$V(t) = V_i \sin\omega' t \tag{12}$$

where V_i is the peak voltage of the source and ω' is the angular frequency. Equ. (12) results in:

$$V(s) = V_i \frac{\omega'}{\left(s^2+\omega'^2\right)} \tag{13}$$

Thus, Equ. (14) is obtained from Equ. (6). This gives the Laplace Transform of the voltage across the resistance R_{eq} that can be used as a system variable to control the heat over the load.

$$V_R(s) = \frac{s\omega'\frac{R_{eq}}{L_{eq}}}{\left((s+\alpha)^2+\omega^2\right)\left(s^2+\omega'^2\right)}V_i \tag{14}$$

V(t) provides energy to compensate the energy dissipated in the resistor. The generated heat has a linear relation with the power injected to the load. So the oscillations do not damp out and the controller operates at around the resonant frequency. Since the system will be driven into resonance, it is advisable that $\omega = \omega'$. Consequently, the switching loss is zero since the current through the switches is zero at the resonant frequency.

Under these conditions, Equ. (14) can be written as:

$$V_R(s) = \frac{s\omega\frac{R_{eq}}{L_{eq}}}{\left((s+\alpha)^2+\omega^2\right)\left(s^2+\omega^2\right)}V_i \tag{15}$$

Doing a partial fractions expansion of Equ. (15) and taking an Inverse Laplace transform, the following is obtained:

$$V_R(t) = V_i \frac{2}{\left(\alpha^2+4\omega^2\right)}\left[\alpha\left(1-\omega e^{-\alpha t}\right)\cos\omega t + \left(2\omega^2 - \left(\alpha^2+2\omega^2\right)e^{-\alpha t}\right)\sin\omega t\right] \tag{16}$$

Equ. (16) contains oscillatory and exponential parts. The oscillatory part contributes to the steady state response while the exponential part contributes to the transient response. Now the power is proportional to the square of the peak voltage, which can be obtained from the envelope function represented by Equ. (17). Equ. (17) contributes to the transient response and leads to the transfer function calculation.

$$V_R(t) = V_i \frac{2}{\left(\alpha^2+4\omega^2\right)}\left[\alpha\left(1-\omega e^{-\alpha t}\right) + 2\omega^2 - \left(\alpha^2+2\omega^2\right)e^{-\alpha t}\right] \tag{17}$$

Arranging the terms of Equ. (17) and factorizing it result in the following:

$$V_R(t) = V_i \frac{2\left(\alpha+2\omega^2\right)}{\left(\alpha^2+4\omega^2\right)}\left[1 - \frac{\left(\alpha^2+\alpha\omega+2\omega^2\right)}{\left(\alpha+2\omega^2\right)}e^{-\alpha t}\right] \tag{18}$$

Above equation can be rewritten as:

$$V_R(t) = V_i\beta_1\left(1-\beta_2 e^{-\alpha t}\right) \tag{19}$$

where:

$$\beta_1 = \frac{2\left(\alpha+2\omega^2\right)}{\left(\alpha^2+4\omega^2\right)} \tag{20}$$

$$\beta_2 = \frac{\left(\alpha^2+\alpha\omega+2\omega^2\right)}{\left(\alpha+2\omega^2\right)} \tag{21}$$

The power is given by:

$$W = \frac{V_R{}^2(t)}{R_{eq}} \tag{22}$$

$$W(t) = V_i^2\frac{\beta_1^2}{2R_{eq}}\left(1-2\beta_2 e^{-\alpha t} + \beta_2 e^{-2\alpha t}\right) \tag{23}$$

The Laplace transform of Equ. (23) gives:

$$W(s) = V_i^2\frac{\beta_1^2}{2R_{eq}}\left(\frac{\left(\beta_2{}^2-2\beta_2+1\right)s^2 + \left(3-4\beta_2+\beta_2{}^2\right)\alpha s + 2\alpha^2}{s^3+3\alpha s^2+2\alpha^2 s}\right) \tag{24}$$

The above equation represents the power over the load as a response to a step $u(s) = 1/s$.

Hence, the plant's transfer function becomes:

$$P(s) = sW(s) \tag{25}$$

$$P(s) = V_i^2\frac{\beta_1^2}{2R_{eq}}\left(\frac{\left(\beta_2{}^2-2\beta_2+1\right)s^2 + \left(3-4\beta_2+\beta_2{}^2\right)\alpha s + 2\alpha^2}{s^2+3\alpha s+2\alpha^2}\right) \tag{26}$$

The transfer function in Equ. (26) supplies the system information needed to design the control strategy and the controllers have been designed based on *P(s)*.

III. Design and Tuning of PID Controllers

A. Designing a Ziegler-Nichols PID Controller

The Proportional-Integral-Derivative (PID) controller is a feedback controller that drives a plant to be controlled by a weighted sum of the error (the difference between the output and a desired set point) and makes the plant less sensitive to changes in the surrounding environment and small changes in the plant.

The PID controller, represented by Fig. 5, is a popular one and is extensively used to improve the dynamic response and to reduce the steady state error. The Derivative controller adds a finite zero to the open loop plant transfer function to improve the transient response. The Integral controller adds a pole at the origin and increases the system type by one

through a reduction in the steady state error to a step function to zero. The PID controller comprises Proportional, Integral and Derivative controls. The PID controller is applied to induction heating systems and is used to control the load power.

The Ziegler-Nichols closed loop tuning is widely used to configure PID controllers for various industrial processes. This method is based on the frequency response of a closed loop system with proportional control only [7]. Ziegler-Nichols tuning can be achieved through the following steps:

- Initially the controller is only set at the proportional mode.
- The gain is initialized with a small value.
- The gain is gradually changed with a small delta and variations in the controlled variables are observed. If the gain is low or high the response is sluggish.
- The gain is increased until the response becomes critically stable. This gain (K_u) is captured together with the corresponding period of oscillations (T_u).
- The gain is adjusted further until a response is obtained that produces continuous oscillations.

The controller gains are specified in Table I. The implementation of such a PID controller is usually done through the following equations:

$$u(t) = K_P\left[e(t) + \frac{1}{T_I}\int_0^t e(t)dt + T_D\frac{de(t)}{dt}\right] \quad (27)$$

Equ. (27) can be written as:

$$u(t) = \left[K_P e(t) + K_I\int_0^t e(t)dt + K_D\frac{de(t)}{dt}\right] \quad (28)$$

To design the PID controller, a set of gains (K_P, K_I, K_D) is determined that improves the transient response of a system by an overshoot reduction and a reduction in the settling time.

While designing through simulation, the controller is set at the proportional mode and the corresponding gain (K_u) at which the output becomes oscillatory for a step input, is determined. This gain is known as the critical gain and the frequency of the oscillation is known as the critical frequency (corresponding to the period of oscillations, T_u). The ZN PID controller parameters (K_P, K_I, K_D) are then determined using the formulae mentioned in Table I. Table IV indicates the values obtained through simulation.

B. Designing a Fine-Tuned PID Controller with a Derivative Filter

One of the most common problems associated with the PID is the synthesis of a derivative action. The ideal derivative has a very high gain, and is susceptible to noise accentuation. Therefore, a PID controller with a first order derivative filter (PIDF) has been chosen instead. PIDF controllers are used in most industrial processes due to its established features such as easy implementation, lower cost

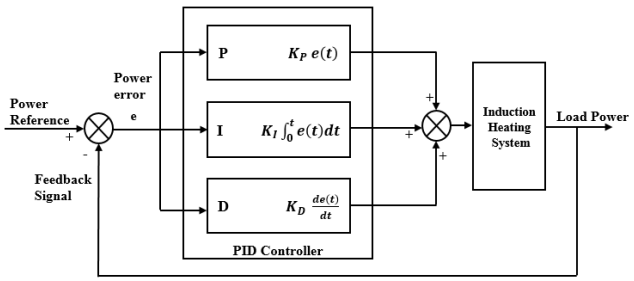

Fig. 5. Block diagram of a PID controller.

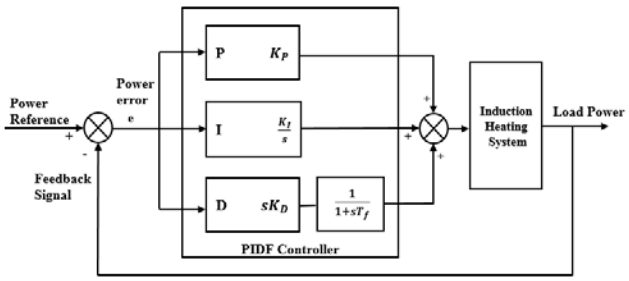

Fig. 6. Block diagram of the PIDF controller.

TABLE I
ZIEGLER-NICHOLS TUNING FORMULAE

Controller	PID
Proportional Gain	$K_P = 0.6K_u$
Integral Time	$T_I = 0.5T_u$
Derivative Time	$T_D = 0.125T_u$
Integral Gain	$K_I = 2.0K_u / T_u$
Derivative Gain	$K_D = 0.125K_uT_u$

and robustness. In general, the performance of a system depends on the efficiency of the controller. Therefore, tuning the PIDF parameters becomes important for system behaviour study. Fig. 6 shows a PIDF controller.

The derivative action of the PIDF controller is represented as $D = \frac{K_D s}{1+sT_f}$, where T_f is the filter time constant, and K_D is the derivative Gain. The controller has proportional gain K_P, integral and derivative times T_I and T_D, and a first-order derivative filter divisor N. Its transfer function is given by:

$$C(s) = K_P\left[1 + \frac{1}{sT_I} + sT_D\frac{1}{1+s\frac{T_D}{N}}\right] \quad (29)$$

The PIDF controller is applied to an induction heating system. The values of K_P, K_I, K_D obtained for the ZN PID controller, are considered as the initial values for tuning. The PID tuning functionality of MATLAB/SIMULINK has been used to tune the PIDF controller and the parameters (K_P, K_I, K_D, N) are adjusted using the tool until a desired set of values is obtained. Table IV indicates the values obtained through simulations. Fig. 7 gives a snapshot of the response while

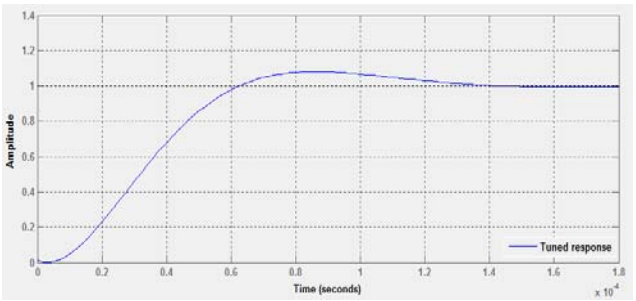

Fig. 7. Step response of a PIDF controller obtained using PID tuning functionality.

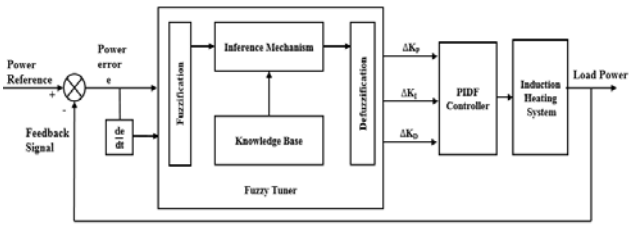

Fig. 8. Block diagram of a fuzzy PIDF controller.

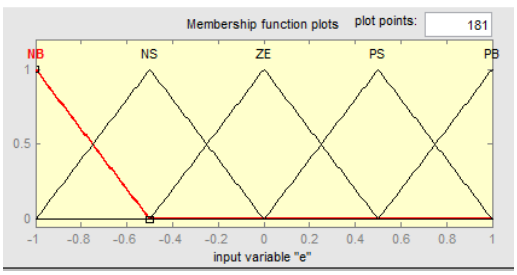

Fig. 9. Membership function for the error (e).

tuning by the tool.

C. *Designing a Fuzzy PID Controller with a Derivative Filter*

Fuzzy logic can be used to implement an effective feedback control mechanism for induction heating systems. The coefficients of a conventional PID controller can be easily tuned using a Fuzzy tuner that comprises a fuzzification interface, a knowledge base, decision making logic and a defuzzification interface. The numerical input values of the fuzzifier are converted into fuzzy values, along with the rule base which are fed into the inference engine that produces the control values. The fuzzifier performs the measurement of input variables, scale mapping and fuzzification. In the fuzzy rule base, various rules are defined depending on their respective problem requirements. Membership functions can be of many forms including triangular, Gaussian, bell-shaped, trapezoidal, etc. The control values are not in a usable form. Therefore, they are converted to numerical output values using the defuzzifier. Fig. 8 shows a block diagram of the proposed fuzzy logic based PIDF controller which modifies the induction heating power output by optimum fuzzy logic tuning. In this case the controller uses two dimensional fuzzy controller models.

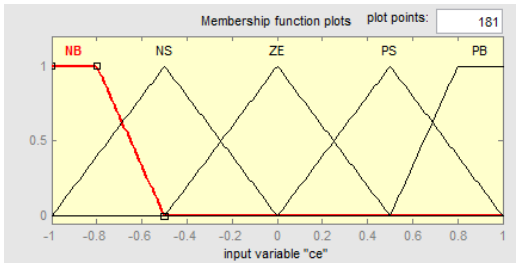

Fig. 10. Membership function for the error change rate (ce).

The general approach to design the controller includes the following steps:

- Defining the input and output variables
- Defining the subset intervals
- Identifying the membership functions
- Setting the rules
- Performing the calculations and adjusting rules.

The fuzzy tuning unit is designed for two input variables and three output variables for achieving the desired level of control. The error (e) and the error change rate ($ce = de/dt$) are the two input variables. The error is the difference between the reference set point and the output. The error change rate (ce) is the difference between the error at time t and (t-1). The three outputs variables (ΔK_P, ΔK_I, ΔK_D) are used to tune the proportional, integral and derivative gains (K_P, K_I, K_D) of the PID controller, respectively. Each of the variables is divided into fuzzy sets. The number of fuzzy sets in each variable is chosen to have the maximum control with the minimum number of rules [8]. To simplify the simulation, this study uses triangular membership functions.

The fuzzy PID control can be expressed as Equ. (30):

$$y(k) = K_P e(k) + K_I \sum_{j=0}^{k} e(j) + K_D[e(k) - e(k-1)] \tag{30}$$

In addition:

$$K_P = K_{P0} + \Delta K_P \tag{31a}$$

$$K_I = K_{I0} + \Delta K_I \tag{31b}$$

$$K_D = K_{D0} + \Delta K_D \tag{31c}$$

$$\Delta K_P = f_1(e, ce) \tag{31d}$$

$$\Delta K_I = f_2(e, ce) \tag{31e}$$

$$\Delta K_D = f_3(e, ce) \tag{31f}$$

K_{P0}, K_{I0}, K_{D0} are the initial values of the PID controller and (ΔK_P, ΔK_I, ΔK_D) are the self-tuned PID parameters obtained by fuzzy reasoning.

The universe of discourse of the input variables is divided into five overlapping fuzzy sets: Negative Big (NB), Negative Small (NS), Zero Error (ZE), Positive Small (PS) and Positive Big (PB). The fuzzy subset is $e = ce = \{NB, NS, ZE, PS, PB\}$. The grade of the membership distribution for the error (e) and the error change rate (ce) are given in Figs. 9-10. The universe of discourse of the three output variables (ΔK_P, ΔK_I, ΔK_D) is divided into five overlapping fuzzy sets: Small (S),

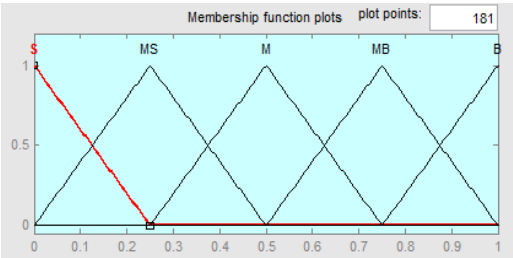

Fig. 11. Membership functions for ΔK_P, ΔK_I, ΔK_D.

TABLE II
FUZZY RULES

e \ ce	NB	NS	ZE	PS	PB
NB	S	S	MS	MS	M
NS	S	MS	MS	M	MB
ZE	MS	MS	M	MB	MB
PS	MS	M	MB	MB	B
PB	M	MB	MB	B	B

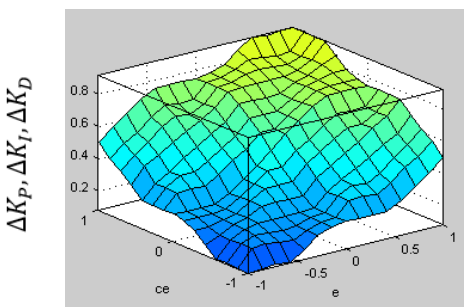

Fig. 12. Control surface between the input and output variables defuzzified by the center of gravity.

Medium Small (*MS*), Medium (*M*), Medium Big (*MB*), Big (*B*), as shown in Fig. 11, with the fuzzy subset {*S, MS, M, MB, B*}.

Experience and knowledge have been leveraged here to build a rule base. The rule base consists of a set of linguistic *IF-THEN* rules containing two antecedences and one consequence, as expressed in the following form:

$R_{i,j,k}$: *IF* $e=A_i$ *and* $\Delta e=B_j$ *THEN* $u=C_k$

where $1 \le i \le 5$, $1 \le j \le 5$, $1 \le k \le 5$. This has resulted in 25 *IF-THEN* rules and the set is represented as a matrix, called a fuzzy rule matrix, as shown in Table II. The decision-making output is obtained using a max-min fuzzy inference, where a crisp output is calculated by the center of gravity (COG) method of defuzzification. In this method the weighted average of the membership function or the center of gravity of the area bounded by the membership function curve is computed as the most typical crisp value of the union for all of the output fuzzy sets:

$$y_c = \frac{\int y\mu_A(y)dy}{\int \mu_A(y)dy} \quad (32)$$

TABLE III
DESIGN SPECIFICATION AND CIRCUIT PARAMETERS

Parameter	Value
R_{eq} (Ω)	2.0
L_{eq} (μH)	47.0
C_r (μF)	0.6
f_r (Hz)	30000
f_s (Hz)	32000
V (V)	230

TABLE IV
K_P, K_I, K_D FOR THE ZN PID, FINE TUNED PIDF AND FUZZY PIDF CONTROLLERS

Controller	ZN PID	Fine Tuned PIDF	Fuzzy PIDF
K_P	11.0×10^{-4}	1.20×10^{-4}	3.25×10^{-4}
K_I	55.977	3.0	4.650
K_D	5.60×10^{-9}	0.95×10^{-9}	4.80×10^{-9}
N	-	243500	243500

where y is the output variable and μ_A the membership function.

The fuzzy inference is designed using the fuzzy toolbox available in MATLAB. Mamdani's fuzzy inference method is used in the proposed fuzzy logic tuner. The surface viewer generates a 3-D control surface with two input variables and three output variables $(\Delta K_P, \Delta K_I, \Delta K_D)$ from the fuzzy inference system as shown in Fig. 12. This controller has the advantage of driving the load at its resonance frequency. Any change in the resonance frequency affects the output power.

A controller is considered to be a robust one if it is capable of tolerating a certain amount of change in the process parameters without making the feedback system unstable.

The system performance is indicated by the performance indices. For a system with a PID controller, there are often four indices that indicate the system performance as defined below [9]:

a. Integral Squared Error (ISE)

$$= \int_0^\infty e^2(t)dt$$

b. Integral Absolute Error (IAE)

$$= \int_0^\infty |e(t)|\,dt$$

c. Integral Time-weighted Squared Error (ITSE)

$$= \int_0^\infty te^2(t)dt$$

d. Integral Time-weighted Absolute Error (ITAE)

$$= \int_0^\infty t\,|e(t)|\,dt$$

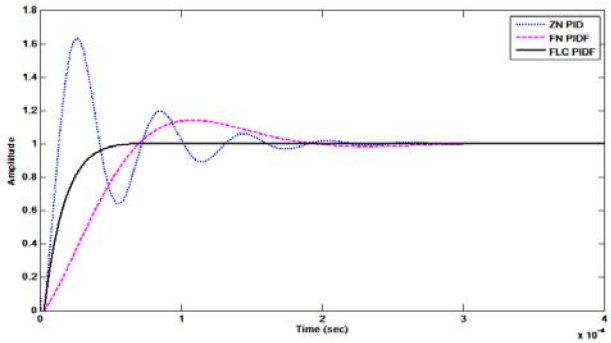

Fig. 13. Step response of an induction heating system with various controller implementations.

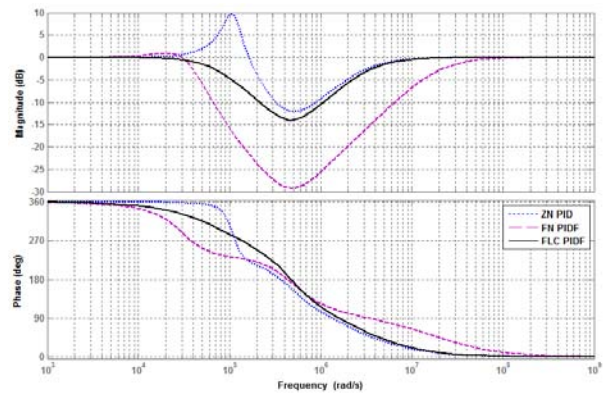

Fig. 14. Frequency response of an induction heating system with various controller implementations.

TABLE V
PERFORMANCE PARAMETERS FOR THE ZN PID, FINE TUNED PIDF AND FUZZY PIDF CONTROLLERS

Parameters	ZN PID Controller	Fine Tuned PIDF Controller	Fuzzy PIDF Controller
Rise Time t_r (sec)	2.14×10^{-10}	6.17×10^{-8}	5.94×10^{-7}
Settling Time t_s (sec)	1.82×10^{-4}	1.78×10^{-4}	4.88×10^{-5}
Overshoot M_p (%)	63.09	14.12	0.15

TABLE VI
ISE, IAE, ITSE AND ITAE FOR THE ZN PID, FINE TUNED PIDF AND FUZZY PIDF CONTROLLERS

Performance Index	ZN PID Controller	Fine Tuned PIDF Controller	Fuzzy PIDF Controller
ISE	4.042×10^{7}	2.518×10^{-5}	2.178×10^{-6}
IAE	7.625×10^{7}	4.458×10^{-5}	2.196×10^{-6}
ITSE	4.051×10^{7}	2.518×10^{-5}	2.178×10^{-6}
ITAE	7.643×10^{7}	4.458×10^{-5}	2.196×10^{-6}

IV. SIMULATION RESULTS AND DISCUSSION

The performances of the ZN PID controller, the Fine Tuned PIDF controller and the Fuzzy PIDF controller have been studied and compared for induction heating systems with a full bridge series resonant inverter. The design specifications and circuit parameters considered in these cases are listed in Table III. These parameters have been leveraged during simulation and experimentation.

All the three controllers have been designed using MATLAB/SIMULINK blocks. For each of the controllers, the set of gains (K_P, K_I, K_D) is determined through simulation. Table IV gives the controller gains obtained through tuning. All of the simulations have been implemented using MATLAB/SIMULINK. Fig. 13 displays the step responses for the given induction heating system with different tuning strategies of the PID controller. The corresponding frequency responses are displayed in Fig. 14. The performance parameters such as the rise time, settling time and overshoot with the ZN PID, fine-tuned PIDF and Fuzzy PIDF controllers for an induction heating system having the given system configuration are presented in Table V. The performance indices of the controllers are listed in Table VI. This comparison gives an idea of the robustness of the proposed controller.

From Table V, it is observed that the overshoots are 63.09% for the ZN PID controller when compared to 14.12% of the Fine Tuned PIDF controller. The Fuzzy PIDF controller drastically reduces the overshoot to 0.15%. The rise time and settling time of the Fuzzy PIDF controller have also been improved when compared to the ZN PID and Fine-tuned PIDF controllers.

TABLE VII
ADDITIONAL SET OF CIRCUIT PARAMETERS

Set of parameters	Parameter	Value
1	R_{eq} (Ω)	3.0
	L_{eq} (μH)	60.0
	C_r (μF)	0.47
	f_r (Hz)	30000
	f_s (Hz)	32000
	V (V)	230
2	R_{eq} (Ω)	40.0
	L_{eq} (μH)	470.0
	C_r (μF)	0.06
	f_r (Hz)	30000
	f_s (Hz)	32000
	V (V)	230

TABLE VIII
K_P, K_I, K_D OF THE FUZZY PIDF CONTROLLERS FOR TWO SETS OF CIRCUIT PARAMETERS

	Fuzzy PIDF Controller for Set 1 (R_{eq} = 3Ω, L_{eq} = 60μH)	**Fuzzy PIDF Controller for Set 2 (R_{eq} = 40Ω, L_{eq} = 470μH)**
K_P	1.18×10^{-4}	3.0×10^{-7}
K_I	2.0	12.68
K_D	2.10×10^{-9}	1.08×10^{-11}
N	243500	243500

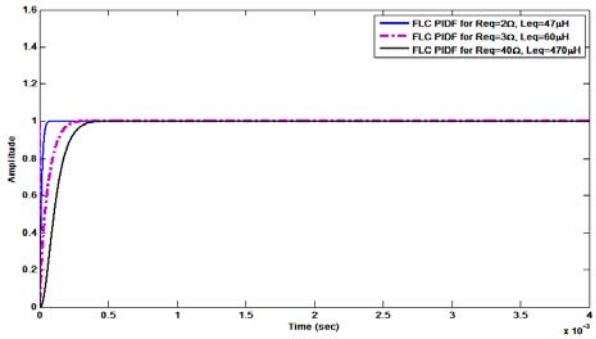

Fig. 15. Step responses of an induction heating system with the Fuzzy PIDF controller for three sets of circuit parameters such as R_{eq} = 2Ω, L_{eq} = 47μH; R_{eq} = 3Ω, L_{eq} = 60μH; and R_{eq} = 40Ω, L_{eq} = 470μH.

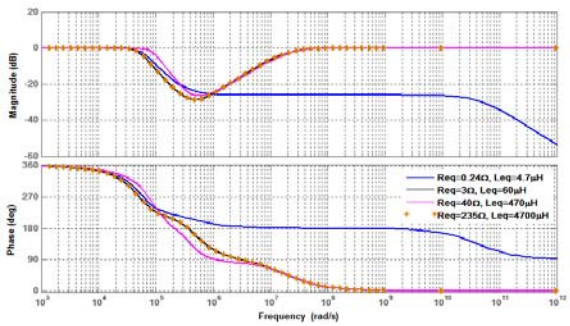

Fig. 16. Bode plots for finding the range of R_{eq}, L_{eq}.

TABLE IX
PERFORMANCE PARAMETERS OF THE FUZZY PIDF CONTROLLERS FOR TWO SETS OF CIRCUIT PARAMETERS

Parameters	Fuzzy PIDF Controller for Set 1 (R_{eq} = 3Ω, L_{eq} = 60μH)	Fuzzy PIDF Controller for Set 2 (R_{eq} = 40Ω, L_{eq} = 470μH)
Rise Time t_r (sec)	1.53×10^{-5}	1.52×10^{-4}
Settling Time t_s (sec)	2.07×10^{-4}	3.21×10^{-4}
Overshoot M_p (%)	0.05	0.02

TABLE X
ISE, IAE, ITSE AND ITAE OF THE FUZZY PIDF CONTROLLERS FOR TWO SETS OF CIRCUIT PARAMETERS

Performance Index	Fuzzy PIDF Controller for Set 1 (R_{eq} = 3Ω, L_{eq} = 60μH)	Fuzzy PIDF Controller for Set 2 (R_{eq} = 40Ω, L_{eq} = 470μH)
ISE	3.3×10^{-6}	3.2×10^{-6}
IAE	3.4×10^{-6}	3.1×10^{-6}
ITSE	3.3×10^{-6}	3.2×10^{-6}
ITAE	3.4×10^{-6}	3.1×10^{-6}

Hence, the Fuzzy PIDF controller outperforms the other two controllers and helps the induction heating system rapidly achieve a set point for the desired power level.

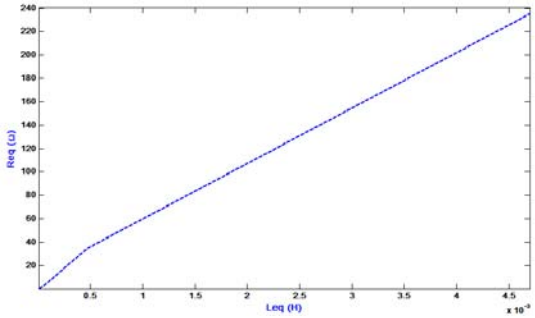

Fig. 17. R_{eq}-L_{eq} profile over the stable region.

The system has been studied with two additional sets of circuit parameters as mentioned in Table VII in order to check the stability of the feedback system for the Fuzzy PIDF controller. The corresponding controller gains obtained through simulations, are given in Table VIII.

Fig. 15 shows the step responses of an induction heating system with the Fuzzy PIDF controller for three different sets of R_{eq}, L_{eq} according to Table III and Table VII. From the responses, it is found that the system remains stable over the chosen range of R_{eq}, L_{eq}.

The performance parameters are mentioned in Table IX and the corresponding ISE, IAE, ITSE and ITAE indices are listed in Table X.

From Tables IX-X, it can be observed that the system with the Fuzzy PIDF controller remains stable against the parameter variations of R_{eq} and L_{eq}. Therefore, the appropriateness of the Fuzzy PIDF controller is obvious.

In order to figure out the region of stability in R_{eq}, L_{eq} for the given Fuzzy PIDF controller, further simulations have been done. Using Bode plots as in Fig. 16, it has been found that the system remains stable for a R_{eq} between 0.24Ω and 235Ω, along with a L_{eq} between 4.7μH and 4700μH.

The variation of R_{eq} has been plotted with the variation of L_{eq}, which results in the profile as shown in Fig. 17. Therefore, for the range in Fig. 17, the system with the Fuzzy PIDF controller remains stable.

V. EXPERIMENTAL VERIFICATION

Results obtained from MATLAB/SIMULINK simulations have been validated through a real time hardware implementation in the laboratory. Fig. 18 shows the experimental setup.

The circuit parameters mentioned in Table III have been considered during experiments. The resonant inverter based induction heating system is realized using four IGBTs IRG4PH40UD and four anti-parallel diodes STTH200L06TV1. The control structure is implemented using a dSPACE DS1104 control card.

The experiment used four IGBTs which operate at a switching frequency that is greater than the resonant frequency so that the ZVS operating condition is achieved

Fig. 18. Experimental set up.

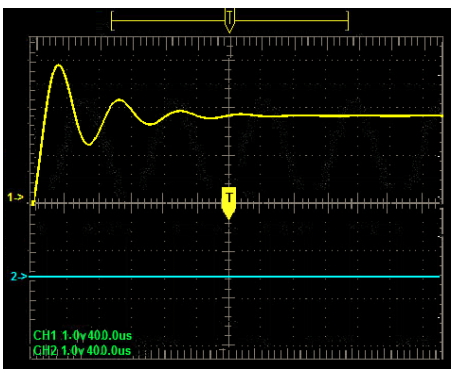

Fig. 19. Step response of the system with the ZN PID controller.

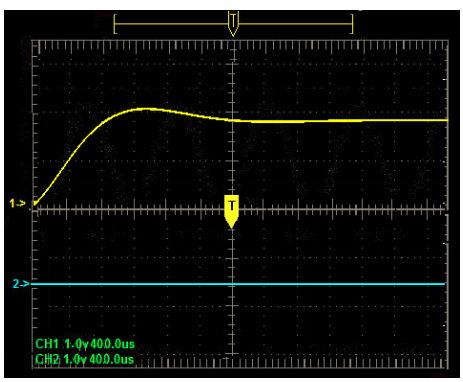

Fig. 20. Step response of the system with the Fine Tuned PIDF controller.

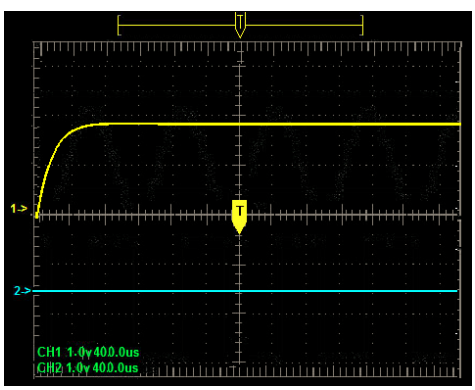

Fig. 21. Step response of the system with the Fuzzy PIDF controller.

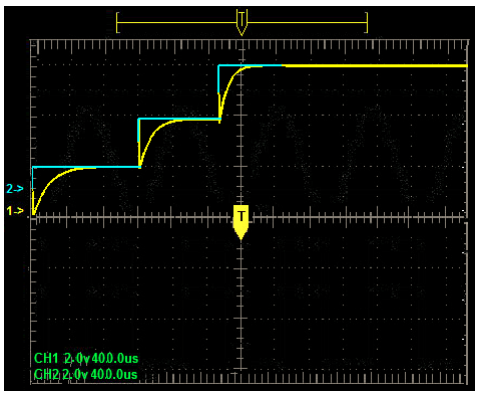

Fig. 22. Dynamic performance of the system with the Fuzzy PIDF controller against set point variations.

and it has achieved satisfactory results [10], [11]. The four anti-parallel diodes help minimize the turn-on loss through ZVS turn-on. Each of the anti-parallel diodes will be in the conduction state before each corresponding IGBT is turned on. In addition, the ZVS will eliminate the capacitive turn-on loss.

The ZN PID, Fine Tuned PIDF and Fuzzy PIDF controllers have been tested for the step input signals, and the corresponding step responses have been plotted. The load is inductive in nature and the output power profiles follow the output current profiles for constant step input voltages. Figs. 19-21 have been plotted for the corresponding current profiles against the step input signals. The time steps and voltage divisions are shown in the figures.

Experiments have also been performed to check the behavior of a closed-loop induction heating system with the Fuzzy PIDF controller against variations of the set points from one steady state to another steady state.

Fig. 22 shows the dynamic performance of such a system for variations of the set points from one steady state to another steady state twice. The response clearly indicates that the system withstands variations of states and gets into the steady state quickly after such variations.

The experimental results are in line with the simulated results and they reinforce the appropriateness of the Fuzzy PIDF controller for the induction heating system studied in this paper.

VI. Conclusion

This paper describes the design and concept of a Fuzzy self-tuning PIDF controller to control the output power of an induction heating system with a full bridge series resonant inverter. Its performance has been compared with that of the ZN PID and Fine-Tuned PIDF controllers. The study shows that the Ziegler-Nichols method results in a higher overshoot, a slower rise time and a slower settling time. The initial controller parameters obtained by Ziegler-Nichols tuning need to be adjusted repeatedly through simulations to get

better and acceptable performance to help design the Fine-Tuned PIDF controller. This gives a smaller overshoot, a better rise time and a better settling time when compared to the ZN PID controller. Nevertheless, the Fuzzy PIDF controller appears to be a better controller performance-wise for the given induction heating system since it results in a minimal overshoot, much faster settling and rise times, and better ISE, IAE, ITSE and ITAE values when compared to the ZN PID and Fine-Tuned PIDF controllers. The reported work presents a systematic approach, which can be easily extended to other inverter topologies. Further work can be done to investigate the feasibility of designing PID controllers using evolutionary algorithms for induction heating systems.

REFERENCES

[1] O. Lucia, P. Maussion, E. Dede, and J. M. Burdio, "Induction heating technology and its applications: Past developments, current technology, and future challenges," *IEEE Trans. Ind. Electron.*, Vol. 61, No. 5, pp. 2509-2520, Sep. 2013.

[2] A. Chakraborty, P. K. Sadhu, K. Bhaumik, P. Pal, and N. Pal, "Behaviour of a high frequency parallel quasi resonant inverter fitted induction heater with different switching frequencies," *Int. J. Electr. Comp. Eng.*, Vol. 6, No. 2, pp. 447-457, Apr. 2016.

[3] A. Chakraborty, T. K. Nag, P. K. Sadhu, and N. Pal, "Harmonics reduction in a current source fed quasi-resonant inverter based induction heater," *Int. J. Power Electron. Drive Syst.*, Vol. 7, No. 2, pp. 431-439, Jun. 2016.

[4] M. H. T. Omar, W. M. Ali, and M. Z. Mostafa, "Auto tuning of PID controller using swarm intelligence," *Int. Rev. Autom. Contr.*, Vol. 4, No. 3, pp. 319-327, May 2011.

[5] P. S. Kumar, N. Vishwanathan and B. K. Murthy, "Multiple-load induction cooking application with three-leg inverter configuration," *Journal of Power Electronics*, Vol. 15, No. 5, pp. 1392-1401, Sep. 2015.

[6] B. Nagarajan and R. R. Sathi, "Phase locked loop based pulse density modulation scheme for the power control of induction heating applications," *Journal of Power Electronics*, Vol. 15, No. 1, pp. 65-77, Jan. 2015.

[7] R. Kumar, S. K. Singla and V. Chopra, "Comparison among some well known control schemes with different tuning methods," *J. Applied Res. Technol.*, Vol. 13, Issue 3, pp. 409-415, Jun. 2015.

[8] X. Yang, C. Song, J. Sun, and X. Wang, "Simulation and implementation of adaptive Fuzzy PID," *J. Netw.*, Vol. 9, No. 10, pp. 2574-2581, Oct. 2014.

[9] P. K. Mohantya, B. K. Sahua, and S. Pandab, "Tuning and assessment of proportional–integral–derivative controller for an automatic voltage regulator system employing local unimodal sampling algorithm," *Electr. Power Compon. Syst.*, Vol. 42, Issue 9, pp. 959-969, May 2014.

[10] A. Chakraborty, D. Roy, T. K. Nag, P. K. Sadhu and N. Pal, "Open Loop Power Control of a Two-Output Induction Heater," *Rev. Roum. Sci. Techn.– Électrotechn. et Énerg.*, Vol. 62, 1, pp. 48-54, 2017.

[11] J. M. Burdío, L. A. Barragán, F. Monterde, D. Navarro and J. Acero, "Asymmetrical voltage-cancellation control for full-bridge series resonant inverters," *IEEE Trans. Power Electron.*, Vol. 19, No. 2, pp. 461-469, Mar. 2004.

Arijit Chakrabarti received his M.Tech. degree in Radio Physics and Electronics from the Institute of Radio Physics and Electronics, University of Calcutta, West Bengal, India. He is presently working as a Consultant for IBM India Private Limited, India. His current research interest includes power electronics, adaptive control, renewable energy, cognitive solutions, artificial intelligence, machine learning, and IoT.

Avijit Chakraborty received his B.Tech. and M.Tech. degrees in Electrical Engineering from the University of Calcutta, West Bengal, India. He is presently working as an Assistant Professor and as the Head of the Department of Electrical Engineering at the Saroj Mohan Institute of Technology, West Bengal, India. In addition, he is doing his doctoral work in the Department of Electrical Engineering, Indian Institute of Technology (ISM), Dhanbad, India. His current research interests include power electronics, electrical machines, power systems, high frequency power electronic converters, and electric drives.

Pradip Kumar Sadhu received his B.E., M.E. and Ph.D. (Engineering) degrees in Electrical Engineering from Jadavpur University, West Bengal, India. He is presently working as a Professor and as the Head of the Department of Electrical Engineering of the Indian Institute of Technology (Indian School of Mines), Dhanbad, India. He has a total of 30 years of experience including 18 years of teaching and research plus 12 years in the industry. He has four granted patents and twenty seven patents that are under process. He has several journal and conference publications at national and international levels. He is the principal investigator of few government funded projects. His current research interest includes power electronics applications, the application of high frequency converters, energy efficient devices, energy efficient drives, computer aided power system analysis, condition monitoring, lighting and communication systems for underground coal mines.